# Activation Energy of Catalysis-Related Domain Motion in *E. coli* Adenylate Kinase

**Yury E. Shapiro* and Eva Meirovitch***

*Mina and Everard Goodman Faculty of Life Sciences, Bar-Ilan University, Ramat-Gan 52900, Israel*

*Received: January 15, 2006; In Final Form: April 2, 2006*

Adenylate kinase from *E. coli* (AKeco), folded into domains CORE, AMPbd, and LID, catalyzes the reaction AMP + ATP ↔ 2ADP. Previous X-ray crystallography and optical solution methods showed that the domains AMPbd and LID, and the conserved P-loop, execute large-amplitude catalysis-related motions. We used $^{15}$N NMR spin relaxation methods to find that the simplified model-free (MF) analysis does not, whereas our general Slowly Relaxing Local Structure analysis does, detect catalytic domain motion. SRLS set for the first time the correlation time for domain motion at $\tau^L{}_\perp = 8.2$ ns, to be compared with $\tau_m = 15.1$ ns for global tumbling. These results were obtained at 303 K. Herein we conduct a temperature-dependent investigation of $\tau^L{}_\perp$ and $\tau_m$ in the range of 288−310 K. We found that the activation energy for global tumbling is $E_a = 16.9 \pm 0.5$ kJ/mol, the hydrodynamic volume of hydrated AKeco is $65.6 \pm 2.1$ nm$^3$, its radius is $2.50 \pm 0.03$ nm, and the number of hydration layers is 1.77. The average $\tau^L{}_\perp$ value decreases from 11 ns at 288 K to 4 ns at 310 K, with activation energies of $29.7 \pm 3.3$, $32.1 \pm 4.3$, and $30.4 \pm 4.3$ kJ/mol for the domains AMPbd and LID, and the catalytic P-loop, respectively. These values are two-to-three times smaller than typical activation energies of enzymatic reactions. Hence kinase catalysis appears not to be controlled by domain motion in the ligand-free enzyme. However, the latter process clearly facilitates important mechanical aspects such as steric recognition and capturing of the AMP and ATP substrates, their proper positioning for phosphorylation, and the release of the ADP product.

## Introduction

Knowledge of protein structure and dynamics is essential for a complete description of biological processes at atomic resolution in general, and enzymatic catalysis in particular.[1−4] NMR spectroscopy is a powerful tool in this context. Although a large number of NMR spin relaxation studies of motions in proteins occurring on the ps−ns time scale,[5−8] and relaxation dispersion studies of dynamic processes occurring on the μs−ms time scale,[9,10] have been reported, a number of fundamental questions associated with the role of protein dynamics in enzymatic catalysis are still unresolved. The view of Pauling[11] that the catalytic power of an enzyme arises from its greater affinity for the transition state than for the ground state is now a fundamental principle of enzymology. It is supplemented by evidence that enzymes properly position reactants to allow thermal motions to carry them efficiently along the reaction coordinate.[12,13] The balance between the dynamic, structural, and stereochemical control of this complex process is largely unknown. In this regard the temperature dependence of dynamic processes (e.g., cf. ref 14), which provides access to the energetics of the dominant motional modes, can help in clarifying the relationship between the various contributing effects. Toward this goal we have undertaken a comprehensive study of the temperature dependence of the ps−ns main chain dynamics of the enzyme adenylate kinase from *E. coli* (AKeco) using NMR spin relaxation methods.[15−17]

AKeco (EC 2.7.4.10) is a particularly interesting enzyme from a dynamical structure−function point of view, as it exhibits catalysis related domain motion.[18] The AKeco molecule consists of a single 23.6 kDa peptide chain folded into the domains CORE, AMPbd, and LID.[19] It catalyzes the phosphoryl transfer reaction $Mg^{2+}$ATP + AMP ↔ $Mg^{2+}$ADP + ADP.[20] While domain CORE is largely preserved structurally during catalysis, the domains AMPbd and LID execute large-amplitude motions between the "open" (Figure 1a) and the "closed" (Figure 1b) forms to configure the active site for substrate binding and dissociate it for product release.[18,21−23] Figure 1a features the ribbon diagram of the (open form) ligand-free crystal structure,[19] and Figure 1b the ribbon diagram of the (closed form) complex of AKeco with the two-substrate-mimicking inhibitor $AP_5A$.[24] The latter has been established as a transition state mimic.[25]

We previously[15] subjected the 14.10 T experimental $^{15}$N $T_1$ and $T_2$ and $^{15}$N−{$^1$H} NOE data of AKeco, and its complex with $AP_5A$, to the commonly used model-free (MF)[26−28] analysis. N−H bond dynamics is characterized with MF in terms of the square of a generalized order parameter, $S^2$, and an effective local motion correlation time, $\tau_e$.[26] For domain motion, which is expected to occur at rates comparable to the rate of global tumbling, the extended version of MF is required. In this case a fast effective local motion described by $S_f{}^2$ and $\tau_f$, and a slow effective local motion described by $S_s{}^2$ and $\tau_s$, are considered, with the slow effective local motion taken to represent domain motion. Although prevalence of domain motion in AKeco was demonstrated both in the crystalline state[21,22] and in solution,[23] the MF $S_s{}^2$ and $\tau_s$ profiles failed to discriminate between the mobile domains AMPbd and LID, and the structurally preserved domain CORE.[15] This was shown by us to be implied by oversimplifications inherent in MF, which ignores the dynamical coupling between the global motion and the slow domain motions, and disregards general features of local geometry.[16] The conclusion that the experimental data exceed the capabilities of MF was reached by applying to the

* Address correspondence to these authors. Y. S.: e-mail shapiro@nmrsgi4.ls.biu.ac.il, phone 972-3-5317926, fax 972-3-5351824. E.M.: e-mail eva@nmrsgi5.ls.biu.ac.il, phone 972−3−5318049.

10.1021/jp060282a CCC: $33.50 
Published on Web 05/20/2006

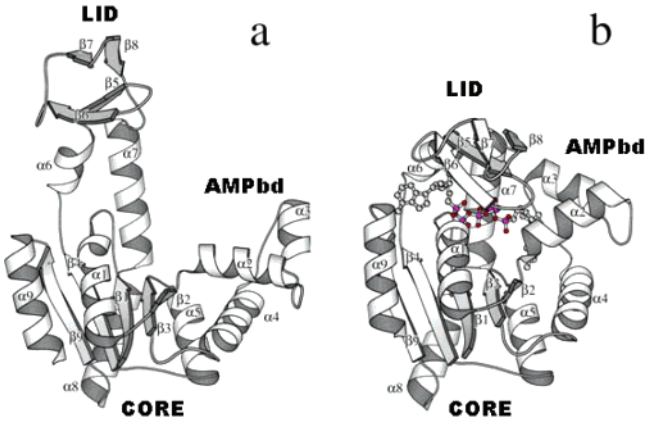


**Figure 1.** Ribbon diagrams of the crystal structures of (a) AKeco and (b) AKeco in complex with the two-substrate-mimic inhibitor $AP_5A$. The figures were drawn with the program Molscript,[63] using the PDB coordinate files 4ake for AKeco and 1ake (complex II) for AKeco*$AP_5A$.

very same experimental data the Slowly Relaxing Local Structure (SRLS) approach of Freed et al. developed originally for ESR,[29,30] and adapted by us recently to NMR spin relaxation in proteins.[31] SRLS accounts rigorously for mode-coupling and general features of local geometry. It constitutes the generalization of MF, yielding the latter in appropriate asymptotic limits.[31,32] By analyzing the $^{15}N$ relaxation data of AKeco acquired at 14.10 and 18.79 T with SRLS we found that order parameters and correlation times associated with the mobile domains AMPbd and LID of AKeco differ significantly from the analogous parameters associated with the structurally preserved domain CORE.[16] Also, the dynamic picture associated with the "open" form was found to be significantly different from that associated with the "closed" form,[17] while in the MF analysis the distinctions were much less conspicuous. For the first time, domain motion in a typical multidomain enzyme was determined experimentally to occur (at 303 K) with correlation time $\tau^L_\perp = 8.2 \pm 1.3$ ns, which is indeed only two times faster than the global motion correlation time, $\tau_m = 15.1 \pm 0.5$ ns.[16]

In proteins, very little is known about the physical nature of local motions in general, and domain motion in particular. Model-free-based NMR spin relaxation studies typically report on near independence of correlation times for local motion on solution temperature[33] and viscosity.[34] Domain motion in $Ca^{2+}$-saturated Xenopus Calmodulin (CaM) was studied recently[35] with MF in the temperature range of 294−316 K. Wobble-in-a-cone motions about the symmetry axis of the axial CaM molecule, characterized in terms of $S_s^2$ and $\tau_s$, were postulated for the N- and C-terminal domains of CaM. Domain motion was found to occur on the same nanosecond time scale as the global tumbling, in disagreement with the mode-decoupling MF approximation. The parameter $S_s^2$ ($\tau_s$) was found to be practically temperature invariant between 294 and 308 K, and to decrease (increase) abruptly upon increasing the temperature from 308 to 316 K. Within the scope of the wobble-in-a-cone motion $\tau_s$ depends on $S_s^2$ and the wobbling rate, $D_w$. The unexpected increase in $\tau_s$ with temperature could be explained by a decrease in $S_s^2$ and an increase in $D_w$. However, at 316 K the value of $D_w$ came out to be slower than $1/(6\tau_m)$, which is physically untenable.

Thus, the physical nature of MF-based local motions in proteins is rather unclear. Therefore exploring internal dynamics with SRLS instead of MF is timely and important, especially when the local motion is associated with functional dynamics. We do so herein by extending out previous 303 K SRLS study of $^{15}N$ spin relaxation in AKeco to a temperature-dependent investigation carried out in the range of 288 to 310 K at 14.10 and 18.79 T. The activation energy for global tumbling, and related physicochemical parameters such as the hydrodynamic volume, the radius, and the thickness of the bound-water shell of the hydrated AKeco particle, were determined. Rates of slow local motion, given by the perpendicular correlation time component, $\tau^L_\perp$, were determined for the mobile domains AMPbd and LID, and the slowly moving catalytic P-loop. The respective activation energies were derived. These values were found to be significantly lower than typical activation energies of enzymatic reactions. This allowed us to infer that domain motion does not control kinase catalysis per se, although it may play an important role in the mechanical aspects of the catalytic process.

## Materials and Methods

**Sample Preparation.** Uniformly $^{15}N$-labeled AKeco was prepared as described earlier.[15] The NMR samples contained 1 mM $^{15}N$-labeled enzyme and 40 mM sodium phosphate buffer in 95% $H_2O$/5% $D_2O$.

**NMR Spectroscopy.** NMR experiments were carried out at 288, 296, 302, and 310 K on Bruker DMX-600 and DRX-800 spectrometers operating at 14.10 and 18.79 T, respectively, using 5 mm $^1H-^{13}C-^{15}N$ triple resonance inverse detection probes, and B-VT-2000 and BTO-2000 temperature control units at 14.10 and 18.79 T, respectively. For each spectrometer, temperature calibrations were carried out with methanol standard. Temperature stability in the course of NMR experiments is estimated at ±0.2 K.

Relaxation times $^{15}N$ $T_1$ and $T_2$ and NOE parameters were measured using inversion recovery, CPMG, and $^{15}N-\{^1H\}$ steady-state NOE experiments.[36−38] For the NOE experiments we used the pulse sequence 1B of ref 38, which features $H_2O$ flip-back pulses to minimize saturation of water. The spectral widths were 1824.5 and 2432.6 Hz in the $F_1$ dimension, and 9615.4 and 12820.5 Hz in the $F_2$ dimension at 14.10 and 18.79 T, respectively. A total of 360 × 2048 complex points were acquired in the $t_1 \times t_2$ dimensions for each time point.

The $^{15}N$ $T_1$ and $T_2$ measurements were performed with a total of 48 and 64 transients per $t_1$ experiment, respectively. For the $T_1$ measurements nine time points were collected, using parametric delays of 15, 127, 247, 367, 487, 647, 807, 1047, and 1407 ms at 14.10 T and 15, 127, 247, 407, 567, 807, 1047, 1367, and 1847 ms at 18.79 T. The experiment was repeated twice for the 15 ms time-points. The time delay between scans was set to 2.6 s. For the $T_2$ measurements eight time points were collected with parametric delays of 8, 16, 32, 48, 64, 80, 104, and 128 ms at both magnetic fields. The time delay between scans was set to 2.2 s. The data were apodized with a cosine (cosine-bell) window function in $t_1$ ($t_2$). Duplicates were used to calculate average values of, and uncertainties in, the measured peak heights. Phenomenological $T_1$ and $T_2$ values and uncertainties were determined by nonlinear least-squares fitting of the experimental data to monoexponential functions.

The $^{15}N-\{^1H\}$ NOE values were measured by using pairs of spectra with and without proton presaturation recorded in an interleaved mode during the recycle delay. A total of 64 and 96 transients per $t_1$ experiment were recorded at 14.10 and 18.79 T, respectively. The delay between scans was 6.0 s at both magnetic fields. The data were processed as described above. The $^{15}N-\{^1H\}$ NOE values were recorded in duplicate, and the replicates were used to determine uncertainties and mean values.

The experimental NMR data were analyzed on Silicon Graphics workstations with the software packages nmrPipe and

modelXY.[39] The previously determined assignments of the AKeco $^1$H-$^{15}$N correlations,[40] complemented and revised in our earlier study,[15] were used.

### Theoretical Background

**The Slowly Relaxing Local Structure Approach.** SRLS is an effective two-body model for which a Smoluchowski equation representing the rotational diffusion of two coupled rotors is solved.[29,30] In SRLS the coupling between the (isotropic) global diffusion frame (C) and the local diffusion frame (M) rigidly attached to the N−H bond is accounted for by a potential $U(\Omega_{CM})$, where $\Omega_{CM}$ denotes the Euler angles between the two frames. $U(\Omega_{CM})$ can be expanded in the full basis set of Wigner rotation matrix elements, $D^L_{KM}(\Omega_{CM})$. If only the lowest order ($L = 2$) terms are preserved, the potential becomes:

$$U(\Omega_{CM})/k_BT = -c^2_0 D^2_{00}(\Omega_{CM}) - c^2_2[D^2_{02}(\Omega_{CM}) + D^2_{0-2}(\Omega_{CM})] \quad (1)$$

where the coefficients $c^2_0$ and $c^2_2$ account for the strengths of the axial and rhombic contributions, respectively. The local ordering at the N−H bond is described by the ordering tensor, **S**, the principal values of which are the ensemble averages:

$$S^2_0 = <D^2_{00}(\Omega_{CM})> \quad (2)$$

and

$$S^2_2 = \langle D^2_{02}(\Omega_{CM}) + D^2_{0-2}(\Omega_{CM})\rangle \quad (3)$$

Axial potentials feature only the first term of eq 1, i.e., $S^2_2 = 0$.

In the absence of an ordering potential the solution of the Smoluchowski equation yields three distinct eigenvalues (or correlation times $\tau_K$; $K = 0, 1, 2$) for the local motion:

$$(\tau_K)^{-1} = 6R^L_\perp + K^2(R^L_{||} - R^L_\perp) \quad (4)$$

where $R^L_{||}$ and $R^L_\perp$ are the relaxation rate constants parallel and perpendicular to the $^{15}$N−$^1$H bond vector, with $R^L_{||} = 1/(6\tau_{||})$ and $R^L_\perp = 1/(6\tau_\perp)$. Each $K$ value leads to its own spectral density component $j_{K=0}(\omega)$, $j_{K=1}(\omega)$, and $j_{K=2}(\omega)$,[41,42] which in this case are Lorentzian functions with widths $(\tau_K)^{-1}$. For magnetic tensors that are axially symmetric in the $M$ frame only $j_{K=0}(\omega)$ enters the measurable spectral density (defined below). Otherwise all three components $j_{K=0}(\omega)$, $j_{K=1}(\omega)$, and $j_{K=2}(\omega)$ determine the measurable spectral density, in accordance with the local geometry. The correlation time for isotropic global motion is $\tau_m = (6R^C)^{-1}$, where $R^C$ denotes the rate of overall rotational reorientation. In general SRLS allows for asymmetric global diffusion tensors, $\mathbf{R}^C$.[30]

In the presence of a local ordering potential the SRLS solution consists of multiple modes, ($j$), expressed in terms of the eigenvalues $1/\tau(j)$ and weighing factors $c_i(j)$ such that:[29,30]

$$j_K(\omega) = \sum_j c_K(j)\tau(j)/[1 + \omega^2(\tau(j))^2] \quad (5)$$

The eigenvalues $1/\tau(j)$ may refer to pure or mixed dynamic modes, in accordance with the parameter range considered. Concise expressions for the SRLS spectral density for dipolar autocorrelation, $J^{dd}(\omega)$, $^{15}$N CSA autocorrelation, $J^{cc}(\omega)$, and $^{15}$N CSA − $^{15}$N−$^1$H dipolar cross-correlation, $J^{cd}(\omega)$, are

$$J^x(\omega) = A(x)j_{K=0}(\omega) + B(x)j_{K=1}(\omega) + C(x)j_{K=2}(\omega) \quad (6)$$

where the coefficients $A(x)$, $B(x)$, and $C(x)$, with $x$ denoting cc, dd, or cd, are given by the trigonometric expressions corresponding to the frame transformations. The NMR relaxation rates associated with N−H bond motion are functions of $J^x(\omega)$ and the magnetic interactions, according to standard expressions for NMR spin relaxation.[43,44] Details on the implementation of SRLS in a data-fitting scheme featuring axial potentials and isotropic global diffusion were outlined previously.[31] This fitting scheme was used in the present study.

### Results and Discussion

The experimental $^{15}$N $T_1$ and $T_2$ and $^{15}$N−{$^1$H} NOE data of AKeco, acquired at 14.10 and 18.79 T at 288, 296, 302, and 310 K, are shown in Figure 2. The $^{15}$N−{$^1$H} NOE is the most sensitive parameter, with the NOE values clearly reduced in the mobile chain regions corresponding to the domains AMPbd and LID, the P-loop ($\beta$1/$\alpha$1), and several additional loops, $\beta$3/$\alpha$5, $\alpha$5/$\beta$4, and $\alpha$8/$\beta$9 (cf. refs 15 and 16 for structural details).

The combined two-field data sets featuring 192 residues were subjected to SRLS analysis. The average experimental errors were 2.5%. The $\chi^2$ probability confidence level was set at 5%, and the $t$-statistics probability confidence level at 20%. The SRLS analysis yields the global motion correlation time, $\tau_m$, the strength of the local potential, $c^2_0$, the local ordering tensor, **S,** and the local diffusion tensor, $\mathbf{R}^L$, both defined in the M frame, and the tilt angle $\beta_{MD}$ between the M frame and the magnetic dipolar frame (parallel to the N−H bond).[31] In this study we focus on the correlation time for global motion, $\tau_m$, and the correlation time for domain motion, $\tau^L_\perp = 1/(6R^L_\perp)$.

**Global Diffusion and Related Physical Parameters.** It was shown previously that conformational averaging implied by large-amplitude domain motion leads to an average structure on the chemical shift NMR time scale.[15] Detailed investigation of the global diffusion tensor, $\mathbf{R}^C$, at 303 K, using the traditional MF methods based on $T_1/T_2$ ratios,[45] led to the conclusion that within a good approximation $\mathbf{R}^C$ is isotropic with $\tau_m = 1/6R^C = 15.1 \pm 0.1$ ns.[15,16] Similar calculations carried out in this study indicated that isotropic global diffusion prevails between 288 and 310 K. The $\tau_m$ values obtained from $T_1/T_2$ ratios were similar to the $\tau_m$ values obtained with an SRLS-based search for minimum $\chi^2$(total)/df(total), where $\chi^2$(total) denotes the global $\chi^2$ value and df (total) the total number of degrees of freedom.[31] The average values, $\langle\tau_m\rangle$, yielded by these different methods are shown in Figure 3a as a function of $\eta/T$, where $\eta$ denotes the (handbook)[46] viscosity of water at the corresponding temperature.

Ideally isotropic global diffusion implies a linear dependence of $\tau_m$ on $\eta/T$, assuming that the temperature dependence of the protein solution viscosity is proportional to the temperature dependence of the viscosity of water. Figure 3a shows that $\langle\tau_m\rangle$ depends linearly on $\eta/T$, with the solid line representing the best fit (with a correlation coefficient of 0.999) of the equation $a_0 + a_1 \times (\eta/T)$. A similar linear dependence of $\tau_m$ on $\eta$/T was observed for the calcium-saturated calmodulin−smMLCKp complex.[14] Thus, in the temperature range investigated, and at a concentration of 1 mM, the hydrated AKeco molecule obeys the Stokes−Einstein law:

$$\langle\tau_m\rangle = (V/k_B)(\eta/T) \quad (7)$$

where $V$ denotes the hydrodynamic volume and $k_B$ is Boltzmann's constant. The value of $V = 65.6 \pm 2.1$ nm$^3$, yielding a radius of $2.50 \pm 0.03$ nm for the hydrated AKeco molecule,

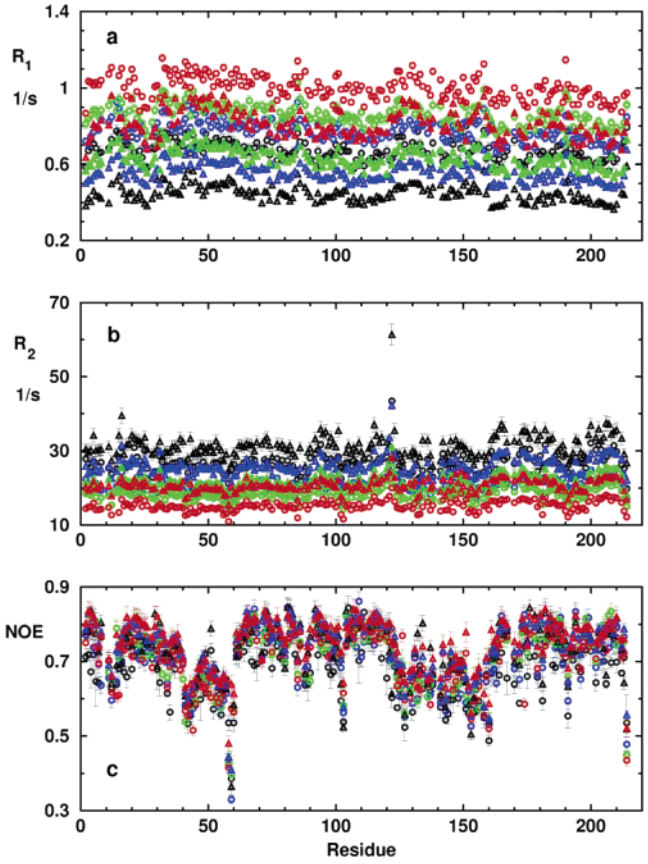


**Figure 2.** Experimental $^{15}$N (a) $R_1 = 1/T_1$ and (b) $R_2 = 1/T_2$ and (c) $^{15}$N−{$^1$H} NOE of AKeco acquired at 288 (black), 296 (blue), 302 (green), and 310 K (red), at 14.10 T (circles) and 18.79 T (triangles), as a function of residue number.

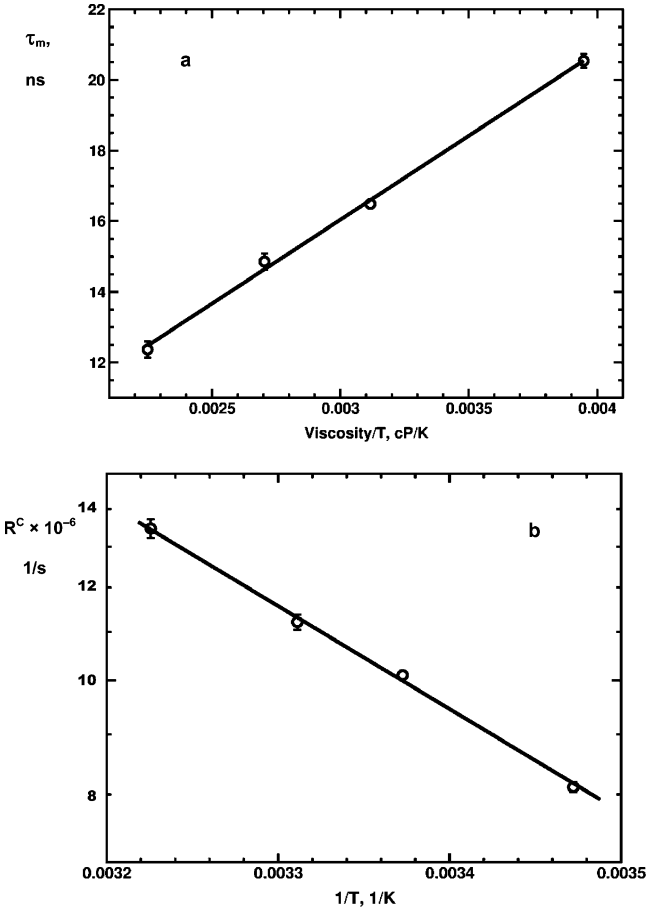


**Figure 3.** (a) Best fit global motion correlation time, $<\tau_m> = 1/(6\langle R^C\rangle)$, as a function of $\eta/T$. The solid line is the best fit of the equation $\tau_m = a_0 + a_1(\eta/T)$. (b) Arrhenius plot of $\langle R^C\rangle$. The solid line is the best fit of the equation $\ln(\langle R^C\rangle) = A - E_a/RT$.

was derived from eq 7. The theoretical hydrodynamic radius of the bare AKeco molecule, calculated as outlined in ref 47 based on a molecular mass of $M = 23\,571$ Da, is $r = 2.01$ nm. The latter value was obtained from the equation $r = 0.07 \times M^{1/3}$ nm, and yields a "bare" volume of 33.02 nm$^3$. The difference of 4.9 Å between the hydrodynamic radii of hydrated and bare protein implies 1220 water molecules per peptide chain, or 5−6 water molecules per amino acid residue, yielding 1.77 layers of bound water (i.e., between a monolayer and a bilayer), assuming a diameter of 2.8 Å for the water molecule. This agrees with 1.70 (1.25) layers of bound water determined for human serum albumin (lysozyme).[48] The values of $\tau_m$ shown in Figure 3a, and the magnitude of the hydration layer, support our previous assertion that at a concentration of 1 mM AKeco prevails predominantly as a monomer in solution.[15]

The Arrhenius plot, $\ln(\langle R^C\rangle)$ versus $1/T$, is shown in Figure 3b. The solid line is the best fit (with correlation coefficient 0.999) of the equation $\ln(\langle R^C\rangle) = A - E_a/RT$, yielding an activation energy of $E_a = 16.9 \pm 0.5$ kJ/mol for the global tumbling of AKeco in aqueous solution. The activation energy for rotational diffusion of water molecules in pure water,[49] and in diluted aqueous solutions of polymers,[50] is also on the order of 17 kJ/mol, in support of AKeco diffusing isotropically as a Brownian particle at 1 mM concentration.

**Domain and P-Loop Motion.** The combined two-field data sets of AKeco acquired at 288, 296, 302, and 310 K were subjected to SRLS analysis, as outlined in detail in refs 16 and 17. The fitting scheme for SRLS used in this study comprises eight models featuring different sets of free variables,[31] in formal analogy with some of the MF fitting schemes where models 1−4 are associated with the original MF formula, and models 5−8 with the extended MF formula. The majority of the CORE residues were fit with model 2, where the set of free parameters includes the strength of the axial potential, $c^2_0$, and the time scale separation between the global and local motions, i.e., the ratio $R^C/R^L$. In some cases model 4, which also includes the exchange term, $R_{ex}$, was used. These calculations yielded local motion correlation times on the order of 20−400 ps (corresponding to $R^C/R^L$ ratios below 0.02), and $c^2_0$ values mostly above 15 (in units of $k_BT$). The relatively large time scale separation and high local ordering potential correspond to fast small amplitude N−H fluctuations, in accordance with the nearly invariant structure of domain CORE.

On the other hand, the AMPbd and LID residues were fit primarily with model 6, where the set of free parameters includes the strength of the axial potential, $c^2_0$, the time scale separation $R^C/R^L_\perp$, the value of $R^L_{||}$ assuming that $R^L_{||} \gg R^L_\perp$, and the diffusion tilt $\beta_{MD}$.[16,17] In some cases model 8, where the set of free parameters also includes the exchange term, $R_{ex}$, was used. These calculations yielded $R^C/R^L_\perp$ on the order of 0.3−0.8, $\tau^L_{||} = 1/(6R^L_{||})$ on the order of tens of picoseconds, average $\tau^L_\perp = 1/(6R^L_\perp)$ values on the order of 4.3−11.0 ns, and $\beta_{MD}$ on the order of 15−20°. As shown previously,[16,17] the physical picture that corresponds to this set of parameters can be rationalized in terms of collective peptide plane motion about the $C^\alpha_{i-1}-C^\alpha_i$ axis. The fact that the AMPbd and LID residues, but not the CORE residues, are engaged in this motion led to the inference that it represents domain motion. The loops $\beta1/\alpha1$ (P-loop), $\beta3/\alpha5$, $\alpha5/\beta4$, and $\alpha8/\beta9$ experience similar collective slow nanosecond motions.[16]

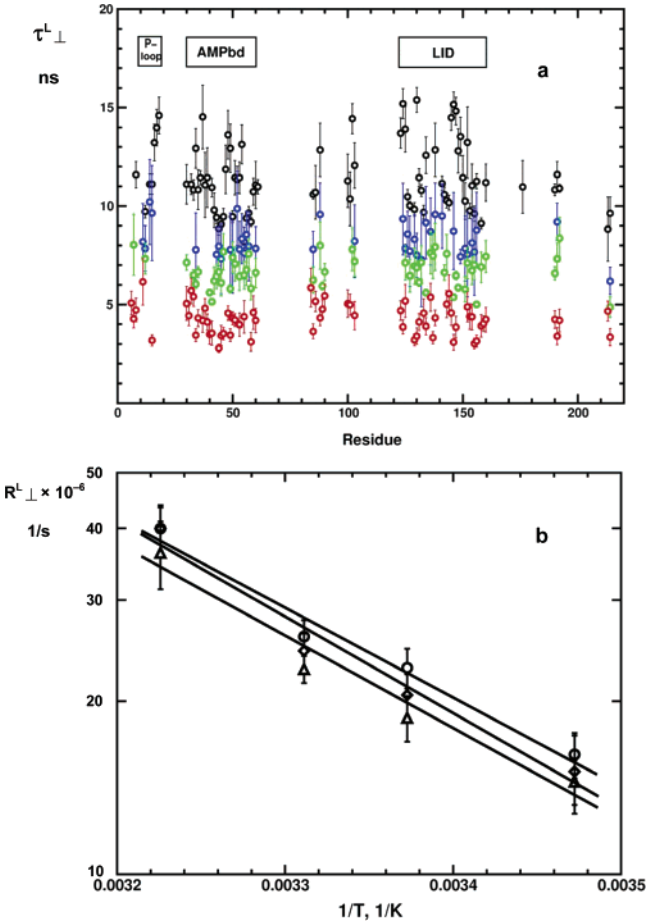


**Figure 4.** (a) Best fit perpendicular local motion correlation time component, $\langle\tau^L{}_\perp\rangle = 1/(6\langle R^L{}_\perp\rangle)$, obtained by applying SRLS to the two-field relaxation data of AKeco acquired at 288 (black), 296 (blue), 302 (green), and 310 K (red) as a function of residue number. (b) Arrhenius plot of $\langle R^L{}_\perp\rangle$ for domain AMPbd (circles), domain LID (triangles), and the P-loop (diamonds). The solid lines correspond to the best- fits of the equation $\ln(\langle R^L{}_\perp\rangle) = A - E_a/RT$.

Figure 4a shows that $\langle\tau^L{}_\perp\rangle$ of the domains AMPbd and LID, the P-loop, and the loops mentioned above decreases significantly as a function of temperature. Figure 4b shows the Arrhenius plots of $\langle R^L{}_\perp\rangle = 1/(6\langle\tau^L{}_\perp\rangle)$ (i.e., $\ln(\langle R^L{}_\perp\rangle$ as a function of $1/T$) for the mobile domains AMPbd and LID, and for the P-loop. The solid lines are best fits (with correlation coefficients of 0.982−0.989) of the equation $\ln(\langle R^L{}_\perp\rangle) = A - E_a/RT$, yielding activation energies of 29.7 ± 3.3, 32.1 ± 4.3, and 30.4 ± 4.3 kJ/mol, respectively.

The average values of $R^C$ ($R^L{}_\perp$) are 8.1, 10.1, 11.2, and 13.5 (15.2, 20.7, 24.3, and 38.7) multiplied by $10^{-6}$ $s^{-1}$ at 288, 296, 302, and 310 K, respectively. This implies time scale separations, $R^C/R^L{}_\perp$, of 0.53, 0.49, 0.46, and 0.35 at 288, 296, 302, and 310 K, respectively. Thus, the coupling between global tumbling and domain motion decreases with increasing temperature (in agreement with the corresponding activation energies). This is an interesting observation, the generality of which is to be investigated in future studies of additional "mechanical" enzymes.

It is in order to compare our results with similar published data. An activation energy of 33 kJ/mol was obtained with time domain reflectometry based on dielectric relaxation for hinge-bending motion in immunoglobulin G (lgG).[51] Activation energies of 21.8 ± 4.2 and 18.8 ± 5.0 kJ/mol were obtained with relaxation dispersion CPMG experiments exploring the μs−ms time scale for segmental motions in the apo (open) and pTppAp-bound (closed) enzyme forms of RNase A, respectively.[52] The latter values are on the same order of magnitude as the activation energy for ligand binding (18.0 ± 15.9 kJ/mol), but three times smaller than the activation energy for ligand release (69.0 ± 5.0 kJ/mol).[52]

The activation energies for nanosecond domain motions in AKeco obtained in this study are two-to-three times smaller than typical "activation energies" of reactions catalyzed by multidomain enzymes, which are on the order of 80−90 kJ/mol.[53,54] This rules out domain motion in the ligand-free enzyme as the rate-determining step, in agreement with the study of Wolf-Watz et al.[55] These authors investigated the linkage between conformational exchange and catalysis of a pair of hyperthermophilic and mesophilic homologues of adenylate kinase (AK). On the basis of biochemical, NMR spectroscopy in general and $^{15}N$ NMR relaxation dispersion methods it has been shown that lid opening in the enzyme−substrate complex before phosphate transfer is the rate-determining step for adenylate kinase catalysis. In particular, it was found that at 20 °C the exchange rate for lid opening is on the order of 44 $s^{-1}$ for the thermophilic AK form and 286 $s^{-1}$ for the mesophilic AK form, while the corresponding $k_{cat}$ values are 30 and 263 $s^{-1}$, respectively.

Our conclusions relate to restricted diffusive motion of the domains AMPbd and LID in the ligand-free enzyme. The conclusions of Wolf-Watz et al.[55] relate to the domain opening motion in the enzyme−substrate complex before phosphorylation. The domains AMPbd and LID may move rapidly (at rates of approximately $1.9 \times 10^7$ $s^{-1}$ at 20 °C, Figure 4b) in the ligand-free enzyme and open slowly (at a rate of 286 $s^{-1}$ at 20 °C) in the enzyme−substrate complex.

In ref 16 we studied the complex of AKeco with the two-substrate-mimic inhibitor $AP_5A$ using $^{15}N$ spin relaxation analyzed with SRLS. In this enzyme form the domains AMPbd and LID (segmentally mobile in the ligand-free enzyme) were not singled out from the domain CORE (segnmentally immobile in the ligand-free enzyme). This agrees with the results of Wolf-Watz et al.[55]

To what extent does the present study contribute to our understanding of kinase catalysis? The rates of domain motion in the ligand-free enzyme were determined for the first time to be on the order of 1.5 to $4.0 \times 10^7$ $s^{-1}$ in the temperature range of 288−310 K (Figure 4b). The activation energy for domain motion in kinases was determined for the first time to be approximately 30 kJ/mol. By comparing the latter with typical enzymatic activation energies a paradigm for using thermodynamic considerations to evaluate flexibility/catalysis relations, i.e., provide information on functional dynamics, has been set forth. Although domain motion in ligand-free AK does not constitute the rate-determining step for adenylate kinase catalysis, one may postulate that it facilitates important *mechanical* aspects of the enzymatic process such as steric recognition and capturing of the AMP and ATP substrates, and their proper positioning for phosphorylation.

The following comments are in order. NMR relaxation dispersion has provided useful information on enzyme catalysis in a number of cases (e.g., refs 55−58). In these studies $k_{ex}$ from relaxation dispersion was compared with $k_{cat}$, hence kinetic considerations were used. In our study activation energies are compared, hence thermodynamic considerations are used.

It should be pointed out that the derivation of activation energies for domain and loop motion in enzymes, and the use of these thermodynamic quantities to determine whether the respective dynamic processes are rate-determining steps of the

catalytic process, is new. Activation energies can be derived with SRLS analysis, which yields the physically expected increase of motional rates with increasing temperature. It cannot be accomplished with model-free[26−28] analysis, which in view of parametrization generates in many cases temperature-independent local motion correlation time profiles, or even reversed trends.[14,59−61] NMR spin relaxation has been used to infer the dynamics/function relationship, based primarily on order parameter considerations.[62]

## Conclusions

In the temperature range of 288−310 K AKeco prevails in solution as a Brownian sphere hydrated with 1.77 monolayers of bound water, tumbling with an activation energy of 16.9 kJ/mol. The rates of nanosecond domain motion are 0.53−0.35 times faster than the rates of global tumbling, indicating decreasing dynamical coupling with increasing temperature. The average activation energy for domain motion in the ligand-free enzyme is 31 kJ/mol. Typical activation energies of enzymatic reactions are significantly higher ruling out this dynamic process as the rate-determining step. Domain motion may still control mechanical aspects of kinase catalysis. Determining rates and activation energies of domain motion in enzymes, and using activation energies to identify the rate-determining step of catalytic processes, constitute new aspects of analysis.

**Acknowledgment.** This work was supported by the Israel−U.S.A. Binational Science Foundation, grant No. 1234/00, the Israel Science Foundation, grant No. 279/03 to E.M., and the Damadian Center for Magnetic Resonance Research at Bar-Ilan University.

## References and Notes

(1) Jencks, W. P. *Catalysis in Chemistry and Enzymology*; Dover: New York, 1987.

(2) Hammes, G. *Biochemistry* **2002**, *41*, 8221−8228.

(3) (a) Benkovic, S. J.; Hammes-Schiffer, S. *Science* **2003**, *301*, 1196−1202. (b) Hammes-Schiffer, S. *Biochemistry* **2002**, *41*, 13335−13343.

(4) Garcia-Viloca, M.; Gao, J.; Karplus, M.; Truhlar, D. G. *Science* **2004**, 303, 186−195.

(5) Kay, L. E. *Nat. Struct. Biol. NMR Suppl.* **1998**, *5*, 513−517.

(6) Ishima, R.; Torchia, D. A. *Nat. Struct. Biol.* **2000**, *7*, 740−743.

(7) Palmer, A. G. *Annu. Rev. Biophys. Biomol. Struct.* **2001**, *30*, 129−155.

(8) Korzhnev, D. M.; Billeter, M.; Arseniev, A. S.; Orekhov, V. Y. *Prog. NMR Spectrosc.* **2001**, *38*, 197−266.

(9) Palmer, A. G.; Kroenke, C. D.; Loria, J. P. In *Methods in Enzymology*; Academic Press: London, UK, 2001; Vol. 339, pp 204−238.

(10) Mulder, F. A. A.; Hon, B.; Mittermaier, A.; Dahlquist, F. W.; Kay, L. *J. Am. Chem. Soc.* **2001**, *123*, 967−975.

(11) Pauling, L. *Nature* **1948**, *161*, 707−709.

(12) Welch, G. R.; Somogyi, B.; Damjanovich, S. *Prog. Biophys. Mol. Biol.* **1982**, *39*, 109−146.

(13) Bruice, T. C.; Benkovic, S. J. *Biochemistry* **2000**, *39*, 6267−6274.

(14) Lee, A. L.; Sharp, K. A.; Kranz, J. K.; Song, X.-J.; Wand, A. J. *Biochemistry* **2002**, *41*, 13814−13825.

(15) Shapiro, Yu. E.; Sinev, M. A.; Sineva, E. V.; Tugarinov, V.; Meirovitch, E. *Biochemistry* **2000**, *39*, 6634−6664.

(16) Shapiro, Yu. E.; Kahana, E.; Tugarinov, V.; Liang, Z.; Freed, J. H.; Meirovitch, E. *Biochemistry* **2002**, *41*, 6271−6281.

(17) Tugarinov, V.; Shapiro, Yu. E.; Liang, Z.; Freed, J. H.; Meirovitch, E. *J. Mol. Biol.* **2002**, *315*, 155−170.

(18) Bennett, W. S.; Huber, R. *Crit. Rev. Biochem.* **1984**, *15*, 291−384.

(19) Müller, C. W.; Schlauderer, G. J.; Reinstein, J.; Schulz, G. *Structure* **1996**, *4*, 147−156.

(20) Noda, L. In *The Enzymes*, 3rd ed.; Boyer, P. D., Ed.; Academic Press: London, UK, 1973; Vol. 8, pp. 279−305.

(21) Vornhein, C.; Schlauderer, G. J.; Schulz, G. *Structure* **1995**, *3*, 483−490.

(22) Müller-Dickermann, H.-J.; Schulz, G. E. *J. Mol. Biol.* **1995**, *246*, 522−530.

(23) Sinev, M. A.; Sineva, E. V.; Ittah, V.; Haas, E. *Biochemistry* **1996**, *35*, 6425−6437.

(24) Müller, C. W.; Schulz, G. *J. Mol. Biol.* **1992**, *224*, 159−177.

(25) Richard, J. P.; Frey, P. A. *J. Am. Chem. Soc.* **1978**, *110*, 7757−7758.

(26) Lipari, G.; Szabo, A. *J. Am. Chem. Soc.* **1982**, *104*, 4546−4559.

(27) Lipari, G.; Szabo, A. *J. Am. Chem. Soc.* **1982**, *104*, 4559−4570.

(28) Clore, G. M.; Szabo, A.; Bax, A.; Kay, L. E.; Driscoll, P. C.; Gronenborn, A. M. *J. Am. Chem. Soc.* **1990**, *112*, 4989−4991.

(29) Polimeno, A.; Freed, J. H. *Adv. Chem. Phys* **1993**, *83*, 89−210.

(30) Polimeno, A.; Freed, J. H. *J. Phys. Chem.* 1**995,** *99*, 10995−11006.

(31) Tugarinov, V.; Liang, Z.; Shapiro, Yu. E.; Freed, J. H.; Meirovitch, E. *J. Am. Chem. Soc.* **2001**, *123*, 3055−3063.

(32) Meirovitch, E.; Shapiro, Y. E.; Liang, Z.; Freed, J. H. *J. Phys. Chem. B* **2003**, *107*, 9898−9904.

(33) Chang, S. L.; Tjandra, N. *J. Magn. Reson.* **2005**, *174*, 43−53.

(34) Zeeb, M.; Jacob, M.; Schindler, T.; Balbach, J. *J. Biomol. NMR* **2003**, *27*, 221−234.

(35) Chang, S. L.; Szabo, A.; Tjandra, N. *J. Am. Chem. Soc.* **2003**, *125*, 11379−11384.

(36) Kay, L. E.; Nicholson, L. K.; Delaglio, F.; Bax, A.; Torchia, D. A. *J. Magn. Reson.* **1992**, *97*, 359−375.

(37) Palmer, A. G.; Skelton, N. J.; Chazin, W. J.; Wright, P. E.; Rance, M. *Mol. Phys.* **1992**, *75*, 699−711.

(38) Grzesiek, S.; Bax, A. *J. Am. Chem. Soc.* **1993**, *115*, 12593−12594.

(39) Delaglio, F.; Grzesiek, S.; Vuister, G. W.; Zhu, G.; Pfeifer, J.; Bax, A. *J. Biomol. NMR* **1995**, *6*, 277−293.

(40) Burlacu-Miron, S.; Perrier, V.; Gilles, A.-M.; Mispelter, J.; Barzu, O.; Craescu, C. T. *J. Biomol. NMR* **1999**, *13*, 93−94.

(41) Freed, J. H. In *Spin Labeling*: *Theory and Applications*; Berliner L. J., Ed.; Academic Press: New York, 1976; p 53.

(42) Freed, H. J.; Nayeem, A.; Rananavare, S. B. *The Molecular Dynamics of Liquid Crystals*; Luckhurst, G. R., Veracini, C. A., Eds.; Kluwer Academic Publishers: Dordrecht, The Netherlands, 1994; Chapter 12, pp 271−312.

(43) Abragam, A. *Principles of Nuclear Magnetism*; Oxford University Press: Clarendon, UK, 1961.

(44) Peng, J. W.; Wagner, G. In *Methods in Enzymology*; James, T. L., Oppenheimer, N. J., Eds.; Academic Press: New York, 1994; Vol. 239, pp 563−595.

(45) (a) Kay, L. E.; Torchia, D. A.; Bax, A. *Biochemistry* **1989**, *28*, 8972−8979. (b) Pawley, N. H.; Wang, C.; Koide, S.; Nicholson, L. K. *J. Biomol. NMR* **2001**, *20*, 149−165.

(46) *Handbook of Chemistry and Physics*, 84th ed.; Lide, D. R., Ed.; CRC Press: Boca Raton, FL, 2004; p 6-3.

(47) Shapiro, Yu. E.; Gorbatyuk, V. Ya.; Levashov, A. V.; Klyachko, N. L. *Biol. Membr.* **1994,** *7*, 277−290.

(48) Rejou-Michel, A.; Henry. F.; de Villardi, M.; Delmotte, M. *Phys. Med. Biol.* **1985**, *30*, 831−837.

(49) Mills, R. *J. Phys. Chem.* **1973**, *77*, 685−688.

(50) Shapiro, Yu. E. *J. Colloid Interface Sci.* **1999**, *212*, 453−465.

(51) Hayashi, Y.; Miura, N.; Isobe, J.; Shinyashiki, N.; Yagihara, S. *Biophys. J.* **2000**, *79*, 1023−1029.

(52) Beach, H.; Cole, R.; Gill, M. L.; Loria, J. P. *J. Am. Chem. Soc.* **2005**, *127*, 9167−9176.

(53) Sampedro, J. G.; Munoz-Clares, R. A.; Uribe, S. *J. Bacteriol.* **2002**, *184*, 4384−4391.

(54) Peinelt, C.; Apell, H.-J. *Biophys. J.* **2004**, *86*, 815−824.

(55) Wolf-Watz, M.; Thai, V.; Henzler-Wildman, K.; Hadjipavlou, G.; Eisenmesser, E. Z.; Kern, D. *Nat. Struct. Mol. Biol.* **2004**, *11*, 945−949.

(56) Nicholson, L. K.; Yamazaki, T.; Torchia, D. A.; Grzesiek, S.; Bax, A.; Stahl, S. J.; Kaufman, J. D.; Wingfield, P. T.; Lam, P. Y. S.; Jadhav, P. K.; Hodge, N. C.; Domaille. P. J.; Chang, C.-H. *Nat. Struct. Biol.* **1995**, *2*, 274−280.

(57) Rozovsky, S.; Jogl, G.; Tong, L.; McDermott, A. E. *J. Mol. Biol.* **2001**, *310*, 271−280.

(58) Wang, L.; Pang, Y.; Holder, T.; Brender, J. R.; Kurochkin, A. V.; Zuiderweg, E. R. P. *Proc. Natl. Acad. Sci.* **2001**, *98*, 7684−7689.

(59) Zeeb, M.; Jacob, M.; Schindler, T. H.; Balbach, J. *J. Biomol. NMR* **2003**, *27*, 221−234.

(60) Chang, S.-L.; Tjandra, N. *J. Magn. Reson.* **2005**, *174*, 43−53.

(61) Vugmeyster, L.; Trott, O.; McKnight, C. J.; Raleigh, D. P.; Palmer, A. G. *J. Mol. Biol.* **2002**, *320*, 841−854.

(62) Osborne, M. J.; Schnell, J.; Benkovic, S. J.; Dyson, H. J.; Wright, P. E. *Biochemistry* **2001**, *40*, 9846−9859.

(63) Kraulis, P. J. *J. Appl. Crystallogr.* **1991**, *24*, 946−995.